Linköping Studies in Health Sciences
Thesis No. 85

MRI Contrast Enhancement using Gd_2O_3 Nanoparticles

Anna Klasson

Linköping University
FACULTY OF HEALTH SCIENCES

Department of Medicine and Health Sciences

Center for Medical Image Science and Visualization

Faculty of Health Sciences
Linköping University, Sweden, 2008

Cover: THP-1 monocytes incubated with nanoparticles of Gd_2O_3 (Petoral et al. Paper 2 in this thesis).

Printed by LiU-Tryck, Linköping, Sweden
ISBN: 978-91-7393-966-9
ISSN: 1100-6013

Abstract

There is an increasing interest for nanomaterials in bio-medical applications and in this work, nanoparticles of gadolinium oxide (Gd_2O_3) have been investigated as a novel contrast agent for Magnetic Resonance Imaging (MRI). Relaxation properties have been studied in aqueous solutions as well as in cell culture medium and the nanoparticles have been explored as cell labeling agents. The fluorescent properties of the particles were used to visualize the internalization in cells and doped particles were also investigated as a multimodal agent that could work as a fluorescent marker for microscopy and as a contrast enhancer for MRI.

Results show that in aqueous solutions, there is a twofold increase in relaxivity for Gd_2O_3 compared to commercial agent Gd-DTPA. In cell culture medium as well as in cells, there is a clear T_1 effect and a distinct increase in signal intensity in T_1-mapped images. Fluorescent studies show that the Gd_2O_3 nanoparticles doped with 5% terbium have interesting fluorescent properties and that these particles could work as a multimodal contrast agent.

This study shows that Gd_2O_3 nanoparticles possess excellent relaxation properties that are retained in more biological environments. Gd_2O_3 particles are suitable as a T_1 contrast agent, but seem also be adequate for T_2 enhancement in for instance cell labeling experiments.

Acknowledgements

First of all, I would like to thank my supervisor, Maria Engström, for all your support, knowledge, encouragement, ideas and patience. Thanks also for the valuable discussions and for all the fun times we have had.

Thanks to my co-supervisors, Kajsa Uvdal and Örjan Smedby, for your support, opinions and valuable ideas.

Special thanks to my collaborators, Maria Ahrén, Eva Hellqvist, Fredrik Söderlind, Henrik Pedersen, Per-Olov Käll, Margaretha Lindroth and Anders Rosén for all your help, your expertise and material supply.

Many thanks to my colleagues and friends at CMIV. I have had a lot of fun times!

Last, but not least, THANKS also to my family for your patience and for always being there for me.

List of Papers

Paper 1: High Proton Relaxivity for Gadolinium Oxide Nanoparticles, Engström M, Klasson A, Pedersen H, Vahlberg C, Käll P-O, Uvdal K. *MAGMA* (2006) 19; 180-186

Paper 2: Synthesis and Characterization of Tb3+ Doped Gd_2O_3 Nanocrystals: A Bifunctional Material with Combined Fluorescent Labeling and MRI Contrast Agent Properties, Petoral RM Jr, Söderlind F, Klasson A, Suska A, Fortin MA, Käll P-O, Engström M, Uvdal K. Submitted to *Journal of Physical Chemistry C*.

Paper 3: Positive MRI Enhancement in THP-1 Cells with Gd_2O_3 Nanoparticles, Klasson A, Ahrén M, Hellqvist E, Söderlind F, Rosén A, Käll P-O, Uvdal K, Engström M. Accepted after minor revision in *Contrast Media and Molecular Imaging.*

Abbreviations

DEG	**Diethylene glycol**
DTPA	**Diethylene triamine pentaacetic acid**
EDX	**Energy Dispersive X-ray**
FCS	**Fetal Calf Serum**
FOV	**Field of View**
HREM	**High Resolution Electron Microscopy**
ICP-SFMS	**Inductively Coupled Plasma Sector Field Mass Spectrometry**
IR	**Inversion Recovery**
MRI	**Magnetic Resonance Imaging**
NMR	**Nuclear Magnetic Resonance**
PEG	**Polyethylene glycol**
PL	**Photoluminiscence**
PMA	**Phorbol 12-myristate 13-acetate**
RF	**Radio Frequency**
SE	**Spin Echo**
SI	**Signal Intensity**
SPIO	**Superparamagnetic Iron Oxide**
TE	**Echo Time**
TEM	**Transmission Electron Microscopy**
TI	**Inversion Time**
TR	**Repetition Time**
XPS	**X-ray Photoelectron Spectroscopy**

Contents

Chapter 1
Introduction

The scientific field where materials smaller than 1 micro-meter, approximately 1-100 nanometers, are studied, is called nanoscience. The word nano is the SI prefix for a billionth, 10^{-9}. Nanoscience is believed to offer many interesting applications in a wide range of fields, from sensor technology to bio-medicine and energy conversion, *e.g.* solar cells. Nanoscaled materials have existed since the beginning of time, but today's huge interest in nanotechnology can be ascribed modern techniques making it possible to actually observe nanometer sized materials. This has made it possible not only to understand how these materials work in different applications, but also to control their function [1].

1.1 Nanoparticles

Nanoparticles are by definition particles in size-range of 1-100 nm. Nanosized particles have a high surface to volume ratio. A considerable fraction of the atoms is located at the surface of the particles. Small particles become crystalline when the atoms are assembled as a three-dimensional periodic array of atoms. A nanocrystal of 1 nm has approximately 100% of its atoms located at the surface while a 10 nm crystal has only about 15% of the atoms at the surface [2]. Several physical

properties will depend on the particle size, such as magnetic, electric and photonic properties as well as chemical reactivity.

1.2 Bio-medical applications

Magnetic nanocrystals are considered for several applications in bio-medicine. Among the most intensely studied are; targeted drug delivery, cancer treatment by hyperthermia and contrast enhancement in magnetic resonance imaging (MRI) [3, 4, 5]. During the last few decades, MRI has become a well established technique for clinical diagnosis. The use of contrast agents to obtain improved images has played a great role for the increased utility of MRI. Paramagnetic or superparamagnetic nanocrystals shorten T_1 and T_2 relaxation times of the ^1H protons in tissues and are therefore considered as MRI contrast enhancers. Today super-paramagnetic iron oxide particles (SPIOs) are routinely used in MRI examinations, but also chelates of, for instance, gadolinium ions.

1.3 Aim

The aim of the work for this thesis was to evaluate nanocrystals of gadolinium oxide, Gd_2O_3, as a contrast enhancing agent for MRI. This was investigated in both H_2O, hydroxylamine buffer, cell culture medium as well as in cells. The Gd nanoparticles were also investigated as a multimodal agent, doped with terbium ions (another lanthanide) for both fluorescent and MRI applications.

Chapter 2

Magnetic Resonance and Relaxation

2.1 Magnetism

Magnetic materials are composed of atoms with valence electrons in the d- or f-shells. Elements with these shells half filled possess a net magnetic moment and builds magnetic materials. These materials have magnetic moments that are aligned parallel, anti-parallel or are randomly oriented. Paramagnetic substances are those that have magnetic properties only when placed in an external magnetic field. This type of magnetism arises in atoms and molecules that have unpaired electrons. When removing the external field, the magnetic effect is lost due to the atoms return to the random orientation. Ferromagnetic substances are magnetically polarized even without an external magnetic field. There are only a few elements that possess ferromagnetic properties, for example iron, cobalt, and nickel. Superparamagnetic materials have a combination of paramagnetic and ferromagnetic properties. When an external magnetic field is applied, these materials show magnetic properties similar to those of ferromagnetic materials. However, when there is no external magnetic field present,

superparamagnetic materials have zero magnetization [6, 7]. The gadolinium ion, Gd^{3+}, has seven unpaired electrons in the valence shell and is therefore suitable as an MRI contrast agent. Gadolinium can be designed in different constellations such as complexes or oxides. Small nanoparticles of gadolinium oxide are said to be superparamagnetic [8], but no unanimous information regarding this could be found in the literature.

2.2 Relaxation

The nucleus of an atom consists of protons and neutrons and has a positive charge, compared to electrons, that are located in orbitals surrounding the nucleus and have negative charge. The nucleus can be considered to rotate around an axis at a constant rate. This rotation is called spin. Nuclear Magnetic Resonance (NMR) is based on the interaction between nuclei that possess spin and an external magnetic field. Nuclear spin is one of several intrinsic characteristics of an atom and depends on the atomic composition. Almost every element in the periodic system has at least one naturally occurring isotope that possesses spin. There are different values for spins, which can be 0, integer or half-integer values. A nucleus has no spin (0) if it has an even atomic weight and an even atomic number. Such nucleus can not interact with magnetic fields and can therefore not be studied using MR. If a nucleus has an even atomic weight and an odd atomic number the spin is said to have an integer value (1,2,3 and so on) and if it has an odd atomic number, the spin is said to be of half-integer value. Nuclei with these values for the spin do

interact with an external magnetic field and can be studied using MR techniques [9].

A charged spinning particle creates an electric current, which, in turn generates a magnetic field. Such nucleus can be considered to be a small bar magnet with magnetic dipoles when the nucleus is placed in a magnetic field (figure 1). Hydrogen has only one proton as a nucleus and is often studied with MRI. The ^{1}H nucleus has spin components of $\pm^{1}/_{2}$ and is the most abundant isotope for hydrogen. Hydrogen is present in many tissues and the water content in the body is close to 80%. Each water molecule spends less than 2% of its time in contact with other molecules in the tissues. The reminder of the time water molecules are free and mobile, which makes ^{1}H a natural choice for probing the body using MRI [10, 11].

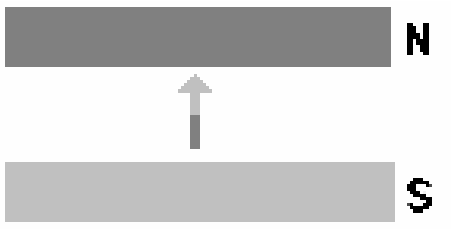

Figure 1. *When placed in an external magnetic field, protons act like bar magnets, lining up to that field.*

When placed in an external magnetic field, hydrogen nuclei either align themselves in the direction of the field, usually referred to as the *z*-direction, or counter-align themselves in the field depending on which spin components they have ($^{1}/_{2}$ or $-^{1}/_{2}$). Thus, the nuclei attain one of two energy states, a lower energy state for aligned nuclei and a higher energy state for counter aligned nuclei. The nuclei are in a state of

equilibrium with a vector for the net magnetization pointing in the z-direction (figure 2). In order to get any information out of this system, the vector needs to be moved away from its equilibrium state. This is achieved by applying a second magnetic field, a radio frequency (RF) pulse that tilts the net magnetization vector away from the z-direction. This RF-pulse is then turned off, whereas the nuclei return to the equilibrium (figure 3). The time it takes for the nuclei to return to the z-direction is governed by an exponential time constant called relaxation time and this is a magnetic resonance phenomenon that is detectable since the tilted vector is still spinning and therefore still induces an electric current. The current from the tilted vector is detected by an RF-receiver that is placed around the examined object. Both the transmitting and receiving of RF-pulses are most often performed by a combined transmit/receive coil that is placed around the object in the MRI-scanner. RF-pulses are repeatedly applied in different sequences and data is

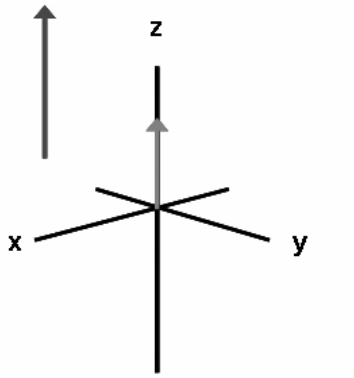

Figure 2. *Net magnetization vector of protons placed in a magnetic field.*

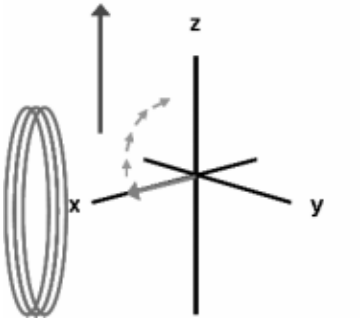

Figure 3. *Longitudinal relax-ation.*
Net magnetization vector returns to the equilibrium state and signal decays in the receiver coil when RF-pulse is turned off.

recorded, analyzed and transformed into images of the examined tissue [12, 13, 14].

There are different kinds of relaxation processes that influence the magnetic resonance signal. Two important ones that are often mentioned for clinical imaging are T_1 and T_2 relaxation. T_1 relaxation, or longitudinal relaxation, is the process that occurs when the spin system is returning to the equilibrium state in the z-direction following an excitation pulse. The protons give up their achieved energy and relax to their original orientation. The return of the net magnetization in the z-direction follows an exponential growth process and T_1 is the time constant that describes this process [10, 12, 15].

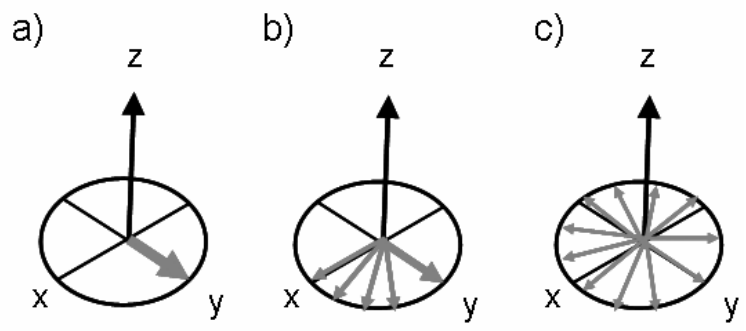

Figure 4. *T_2-relaxation process in the x-y plane of the spin system. a) shows net magnetization vector directly after RF-pulse, b) shows the transverse relaxation starting after RF-pulse is turned of and c) shows the relaxed transverse magnetization.*

When exciting a spin system it initially behaves coherent, which means that the magnetization of all the components in the system are in phase in the same direction. There is also a magnetization in the x-y plane of the spin system. Directly

after an excitation pulse, all the protons precess in phase and their individual magnetic moments will collectively contribute to the transverse magnetization vector. The magnetization will dephase in the x-y plane when the externally applied RF-pulse is turned off. This transverse relaxation, or T_2 relaxation, is described as the time required for the transverse components to decay (figure 4). When the longitudinal magnetization has reached its equilibrium, there can be no transverse magnetization and the decay of the signal in the x-y plane is therefore faster than the decay of the longitudinal magnetization along the *z* axis. This means that T_2 relaxation time is always less than or equal to the corresponding T_1 time [10, 12, 13, 15].

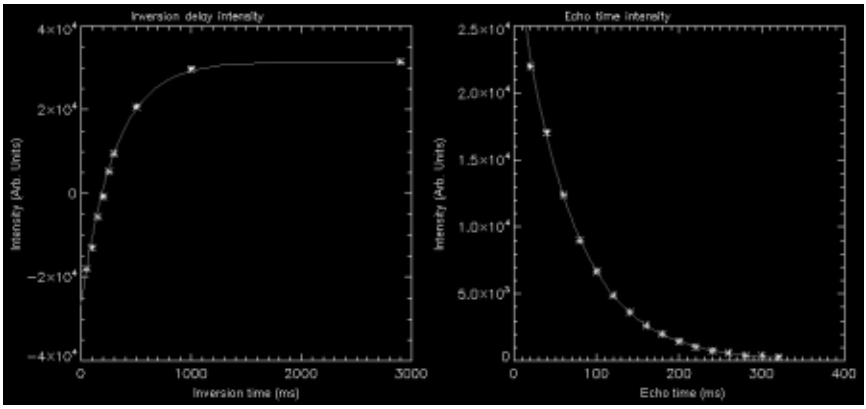

Figure 5. *T_1 relaxation curve after inversion pulse (left) and T_2 relaxation curve after excitation pulse (right), show signal intensity of measured samples.*

T_1 and T_2 behavior can be described as curves in figure 5. Directly following an RF-pulse, the magnetization of the protons changes. This causes a change in signal intensity of the examined tissue. After an inversion pulse, the longitudinal magnetization is turned to the –*z* axis and this can be observed in the T_1 relaxation curve of figure 5. After an

excitation pulse a transverse magnetization is created. When the excitation pulse is turned off, the magnetization returns to equilibrium and the signal detected by the receiver coil decays.

2.3 T_1-weighted pulse sequences

Spin echo: Conventional spin echo techniques have been the most common method for acquiring T_1-weighted images. Using optimized spin echo sequences, high quality images with T_1-weighting can be obtained within a few minutes. A spin echo is formed by an excitation pulse and one or more refocusing pulses. Usually the excitation pulse is 90˚ and the refocusing pulse 180˚. Refocusing pulses is used to rotate the dispersing excited spins in the transverse plane so that the magnetization vectors will rephase. T_1-weighted spin echo imaging is perhaps the most robust and the most forgiving technique. Generally the repetition time (TR) is 600 ms or less for T_1-weighted images, but shorter TRs are needed with decreasing field strengths. One limitation is that only a few slices can be acquired per TR, but with modern software this limitation is not significant because several sets of images can be programmed simultaneously and acquired sequentially. The echo time (TE) is at least as critical as the TR for obtaining optimal contrast in T_1 weighted spin echo images. During the TE, transverse magnetization decays depending on the T_2, reducing the signal-to-noise ratio and introducing T_2 contrast to the images. T_2 contrast works in opposition to T_1 contrast for most tissue comparisons and is therefore generally undesirable on T_1-weighted images. T_2 contrast can be minimized using the shortest possible TE [15].

Inversion recovery: Inversion recovery (IR) pulse sequences can be used to achieve stronger, more flexible T_1 contrast on, for example, spin echo images. Spin echo inversion recovery images are acquired by preceding each excitation pulse with an inversion pulse. When imaging tissues with variations in T_1 relaxation times, this can be manipulated using such preceding inversion recovery pulse prior to the excitation pulse since the inversion pulse will flip the longitudinal magnetization from the +z axis to the –z axis. Before the excitation pulse is applied, a time delay is provided to allow the inverted magnetization to recover towards its equilibrium value. This time between an inversion recovery pulse and the excitation pulse is called inversion time (TI). Tissues with different T_1 values recover at different rates, creating a T_1 contrast among them. The excitation pulse then converts the differences in the longitudinal magnetization into differences in the transverse magnetization, which produces signal that form an image with T_1-weighted contrast. Most IR pulse sequences require a relatively long TR (e.g. TR = 2-11 s) to preserve the contrast established by the IR module and therefore the acquisition time can become long. Inversion recovery pulse sequences have many applications and are widely used in clinical practice and in addition to produce images, IR can also be used to generate T_1 maps [16].

2.4 T_2-weighted pulse sequences

Spin echo: Like T_1-weighted imaging techniques, T_2-weighted images can be obtained via the spin echo (SE) technique, which was common in the first decade of clinical MRI. This technique provides acceptable T_2 contrast for most tissues.

However, the number of images that can be acquired per TR decreases with long TE and therefore there is a practical limit to the TE that can be used in clinical practice before the acquisition times are unacceptably long. The long survival of the relatively inefficient T_2-weighted SE images in clinical practice has been due to the lack of acceptable alternatives. However, in recent years, other techniques have been developed for T_2-weighted imaging.

Gradient Echo: Gradient echo pulse sequences consist of an excitation pulse followed by measurement of a gradient echo. Magnetic field gradients are part of the fundamental principle used to detect the location of MR signal sources. In a homogenous magnetic field, without applying field gradients, protons precess at the same frequency regardless of their location. Supplying an extra magnetic field that decreases gradually from one end of the magnet to the other, the resulting total magnetic field is strong in one end and weak at the other. The precession frequency of protons is proportional to the magnetic field, to which they are exposed, and because the magnetic field gradient produces variation in this frequency, the protons at one end of the magnet precess slower than on the other end. If an RF-pulse is transmitted into a tissue when a gradient is present, not all protons in the tissue are excited. Only tissue in which the protons precess at appropriate frequency are excited. Thus, only a limited part of the tissue is excited and through this you get information from where in the tissue the signal is derived from. This process of encoding the location of protons based on their positions along an applied gradient during measurement is called frequency encoding. This frequency encoding gradient

can be applied in certain ways to create gradient echoes, which are measured and used when transforming the signals to images [15].

Chapter 3
Contrast Agents in MRI

In spite of the excellent soft tissue contrast of MRI, the application of contrast agents in clinical imaging was discussed more than 15 years ago [17]. Contrast agents in MRI can for example be administered to further enhance tissue contrast, to characterize lesions and to evaluate perfusion and blood flow abnormalities [18].

3.1 Contrast Mechanisms

Contrast mechanisms in MRI are indirect effects of the contrast agent's ability to alter the hydrogen relaxation times, T_1 and/or T_2, in the tissue, thereby influencing the signal intensity and the image contrast. One requirement for an efficient MRI contrast agent is therefore the ability to interact with hydrogen. The agent work by altering the relaxation times of hydrogen nuclei that come into close contact with the contrast agent. Single, unpaired electrons have magnetic dipole moments that are over 650 times stronger than that of single, unpaired protons. Because of this, the magnetic effects of unpaired electrons dominate the magnetic effects of the atom. The number of unpaired electrons in the outer shell of an atom is therefore important for determining the effect the particular atom has as a relaxation contrast agent. Elements

with the highest numbers of unpaired electrons and also the longest electron spin relaxation times will have the strongest magnetic relaxation effects on hydrogen. The effect of paramagnetic contrast agents on tissue relaxation rates is in direct proportion to the concentration of the agent as shown in formula

$$1/T_{1/2(\text{observed})} = 1/T_{1/2(\text{inherent})} + r_{1,2} * C$$

where inherent stands for the tissue relaxation properties without contrast agent and observed stands for the relaxation properties with contrast agent, $r_{1,2}$ are the relaxivities and C is the concentration of the agent [11].

MRI with contrast agents is now a well established technique for clinical diagnosis and the use of such agents to obtain improved images has played a great role for the increased utility of MRI. Today there are mainly two contrast agents used in MRI; superparamagnetic iron oxide particles (SPIOs) and paramagnetic chelates. Different chelates of Gd^{3+} are the most commonly used agents. The Gd^{3+} ion is strongly paramagnetic due to its seven unpaired f-electrons. However, Gd^{3+} chelates have low relaxivity compared to what is theoretically possible and they are not very selective [9]. There is a demand for new, more efficient and tissue specific agents that could be used as molecular markers and magnetic tracers.

3.2 Lanthanides and gadolinium

In 1974, the Finnish chemist and Professor J. Gadolin, examined a recently discovered mineral, gadolinite, and from this mineral he isolated a new oxide, yttria (named after the

small village Ytterby in the Swedish archipelago outside Stockholm where gadolinite once was found). Yttria was shown to content yttrium (Y), terbium (Tb), erbium (Er), ytterbium (Yb), scandium (Sc), holmium (Ho), thulium (Tm), gadolinium (Gd), dysprosium (Dy) and lutetium (Lu). These elements are some elements of the lanthanides, or rare earth metals [19, 20]. Gadolinia, the oxide of gadolinium, was discovered from yttria in 1886 by the French chemist Paul Émile Lecoq de Boisbaudran. In nature Gd is present only in chemical compounds and in mixtures with other rare earth metals. Gd can be separated chemically and the metal is silver white, shining and soft. It has been found to be ferromagnetic up to room temperature and thereafter it is paramagnetic. Because of its magnetic properties it has come to medical use in MRI [21].

Chapter 4
Cell labeling

4.1 Cell labeling with nanoparticles

There are several methods to label different cell types with magnetic nanoparticles [22]. SPIOs are most frequently used for cell labeling experiments. However, they usually generate negative contrast, even though there are known methods and MRI sequences that can generate positive contrast from SPIOs [3, 23, 24]. A drawback with negative contrast agents is that they create signal voids in the images and therefore the contrast could be difficult to detect. Loss of signal in tissue pathologies is not unusual and the presence of such voids makes it complicated to discriminate between the contrast, tissue and image artifacts. A particulate agent that generates positive contrast could be an important complement to SPIOs. For this, Gd_2O_3 nanoparticles possess desirable properties [25].

Small size iron oxide particles (<100 nm) facilitates transport across cell membranes and labeling is usually performed by incubating the cells of interest with the contrast agent *in vitro* so that they can be monitored using MRI. The uptake of the contrast agent occurs through phagocytosis/endocytosis and

this has been used to image, for instance, atherosclerosis and other inflammatory processes [26].

4.2 THP-1 cells

In this thesis work, the cell line THP-1 was used. It is a monocytic cell line derived from the peripheral blood from a one year old male with acute monocytic leukemia. THP-1 monocytes have Fc and C3b receptors and lack surface and cytoplasmic immunoglobulins. They produce lysozymes and are believed to be phagocytic [27, 28]. If treated with phorbol esters, THP-1 monocytes can differentiate into macrophage like cells, which mimic native monocyte-derived macrophages. Differentiated THP-1 cells behave more like these native monocyte-derived macrophages than other well established cell lines, such as U937, HL-60 and HELA [29].

These THP-1 cells are easy to keep in culture and they are very tolerable and this is the reason why they were chosen to be studied in this work.

Chapter 5
Fluorescence

5.1 Fluorescence physics

In fluorescence microscopy, the specimens of interest are usually treated with special reagents to accomplish the fluorescent signals. The molecules of these reagents are able to absorb light for an extremely short time and then emit the light. The emitted light is shifted to a longer wavelength than the excitation (absorption) wavelength, for example, blue light is absorbed and green light is then emitted immediately afterwards. Green is changed to yellow, yellow to red and so on. This shift is termed Stokes shift after its discoverer. In fluorescence, the wavelength of the emitted light is about 20 to 50 nanometers longer than absorbed exciting light. Fluorescence molecules can only absorb light of a certain wavelength. Each of the various fluorochromes exhibits its own, specific excitation spectrum depending on the internal structure of the fluorescence molecules and their surroundings. Furthermore, not every photon is absorbed, but only a fraction of incoming photons. The total energy of absorbed fraction of photons is not entirely converted to emitted light. Good fluorescence probes feature a high quantum yield, which is describing the ratio of the emitted to the absorbed photons. This is, for instance, very useful for

microscopy. Nowadays, fluorescence methods have made it possible to specifically couple the fluorescence molecules with biological substances, for instance antibodies and thereby there are probes that can target specific structures and tissues of interest [30, 31].

5.2 Applications

Fluorescence microscopy, as well as other optical imaging techniques, are well established and highly developed for *in vitro* and *ex vivo* applications in molecular and cellular biology. An extension of this toward non-invasive *in vivo* imaging represents an interesting future for extracting biological information from living subjects [32]. One approach to *in vivo* molecular MRI could be the design of a multimodal contrast agent with optical and magnetic properties for dual imaging. Such agent could be useful in preoperative diagnosis and in intra-operative surgical resection of brain tumors or other lesions [33, 34]. For this purpose, lanthanides (rare-earths) possess suitable properties. Rare-earth doped nanoparticles are promising materials for fluorescent labeling, as they usually have narrow emission spectra, long lifetimes, and minimized photobleaching. Pure gadolinium oxide is fluorescent with an emission spectrum showing a broad band centered at 530 nm. Doped with for instance 10% europium, the emission spectrum shows a narrow peak at 600-620 nm [35]. Other lanthanide ions, such as for instance Tb^{3+} and Yb^{3+}, can also be of consideration when doping rare-earths like Gd_2O_3 nanoparticles.

5.3 Fluorescence studies in this thesis

In this work the original idea was, however, to use the fluorescent properties of undoped gadolinium and see if we could detect if the cells had taken up particles when incubated with these for a certain time. We then achieved images of Gd_2O_3-DEG particles lighting up cell organelles

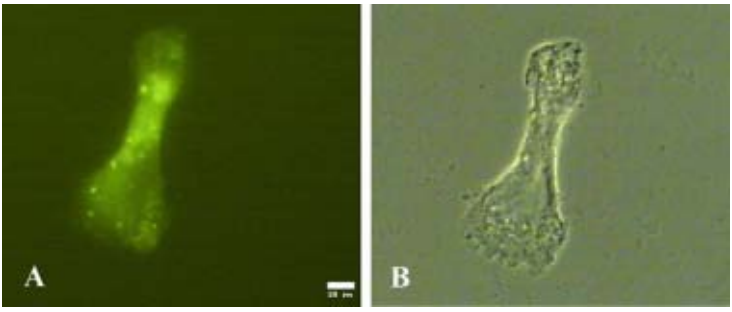

Figure 6. *A) shows fluorescence microscopy image of THP-1 cell incubated with Gd_2O_3 nanoparticles. B) shows confocal microscopy image of the same cell.*

(probably lysosomes or endosomes) inside the cells (figure 6). This experiment then lead to an extended collaboration with the department of Physics, Chemistry and Biology at Linköping University to visualize the weakly fluorescent gadolinium particles doped with another, more strongly fluorescent lanthanide (terbium), and monitor them inside cells. We also wanted to investigate the relaxation properties of these particles and these studies are described in Paper 2 of this thesis.

Chapter 6
Papers

Paper 1 – High Proton Relaxivity for Gadolinium Oxide Nanoparticles.
Paper 2 – Synthesis and Characterization of Tb^{3+} doped Gd_2O_3 Nanocrystals: A Bifunctional Material with Combined Fluorescent Labeling and MRI Contrast Agent Properties.
Paper 3 – Positive MRI Contrast Enhancement in THP-1 Cells with Gd_2O_3 Nanoparticles.

6.1 Summary of papers

Paper 1
High Proton Relaxivity for Gadolinium Oxide Nanoparticles.

Nanosized materials of Gd_2O_3 can provide high contrast enhancement in MRI and nanoparticles are promising candidates for molecular imaging because they convey the possibility of high relaxivity per molecular binding site. In this study, we investigate proton relaxation enhancement by ultrasmall (5-10 nm) Gd_2O_3 nanocrystals. Nanocrystals coated with diethylene glycol (DEG) were syntesized, characterized by X-ray photoelectron spectroscopy (XPS), and

investigated by MRI relaxometry. Relaxivity of Gd_2O_3 was compared with gadolinium chelates in clinical use today.

Particle synthesis: Gadolinium oxide nanocrystals were synthesized by the polyol method in two different ways. A mixture of NaOH, DEG and either $Gd(NO_3)_3$ or $GdCl_3$ was heated to 140˚C and when reactants had dissolved, the temperature was raised to 180˚C and held constant for 4 h, yielding a dark yellow colloid.

XPS: The chemical composition of the nanocrystals was investigated by X-ray photoelectron spectroscopy.

Relaxivity measurements: Samples of Gd_2O_3-DEG and Gd-DTPA (Magnevist®) were prepared in 10 mm NMR test tubes with H_2O, 1 M hydroxylamine buffer ($NH_2(OH)/NH_3(OH)^+$) and in RPMI 1640 cell culture medium (Gibco, Invitrogen) in concentrations of 0.1 to 1.6 mM. During measurement the tubes were immersed in a bowl with saline and pH of the samples were measured by a Metrohm 744 pH meter and also checked by pH-indicator strips (Merck). T_1 and T_2 relaxation times were measured with a 1.5T Philips Achieva clinical scanner using the head coil. A 2D mixed multiecho SE interleaved with a multiecho IR sequence was used for the measurements. Imaging parameters were varied to minimize the standard deviations in relaxation time calculations. Gd contents in nanoparticle stem solutions were determined by inductively coupled plasma sector field mass spectrometry (ICP-SFMS) at Analytica AB (Luleå, Sweden).

Relaxivity results and discussion: Gd_2O_3-DEG nanoparticles induced higher proton relaxivities compared to Gd-DTPA (relaxivity constants are given in table 1). The relaxivities due to the nanoparicles were twice that of the chelate. This is, to our knowledge, the first time relaxation behaviour for such Gd_2O_3 nanoparticles have been reported. Another interesting observation was the marked T_1-reducing

effect and simulated signal increase at low concentrations (~<0.7 mM). The concentration range below 0.6 mM in plasma is most relevant for clinical use. At the recommended dose of Magnevist, 0.1 mmol/kg, the detected plasma concentration of Gd is 0.6 mM at 3 min. after injection.

Table 1. *Relaxivity constants (r_1, r_2) in s^{-1} mM^{-1}, standard deviation (SD), and p values for Gd-DTPA and Gd_2O_3-DEG in H_2O. buffer and cell culture medium (RPMI 1640) measured at 1.5T, 21-23˚C.*

	r_1	SD	p	r_2	SD	p	pH
H_2O							
Gd-DTPA	4.7	±0.1	<0.0001	5.3	±0.2	<0.0001	5.4
Gd_2O_3-DEG(1)	9.2	±0.3	<0.0001	11.3	±0.4	<0.0001	6.3-7.2
Buffer							
Gd-DTPA	5.6	±0.3	<0.0001	6.2	±0.3	<0.0001	7.2
Gd_2O_3-DEG(2)	9.8	±0.5	<0.0001	11.9	±0.7	<0.0001	7.4
RPMI							
Gd-DTPA	5.1	±0.1	<0.0001	6.4	±0.1	<0.0001	7.3
Gd_2O_3-DEG(1)	13.2	±0.7	<0.0001	24.6	±2.3	0.0003	7.3
Gd_2O_3-DEG(2)	13.9	±0.8	<0.0001	22.3	±1.9	0.0017	7.3

Paper 2

Synthesis and Characterization of Tb^{3+} doped Gd_2O_3 Nanocrystals: A Bifunctional Material with Combined Fluorescent Labeling and MRI Contrast Agent Properties.

Molecular imaging with aid of targeted contrast agents like fluorescent probes has been improving in the past decade regarding, for instance, detection limits, imaging modalities and engineered functionality. Recently, the development of

engineered nanoparticles with multifunctional features has emerged. Rare-earth based nanoparticles are promising types of luminescent and ion-doped lanthanide oxide nanoparticles are highly photostable, exhibit long luminescence lifetimes and narrow emission bands. In this study, rare-earth oxide Gd_2O_3 nanoparticles doped with Tb_3^+ ions were synthesizised and capped with different organic acids and further, polyethylene glycol (PEG)-containing molecules were coupled to the acids. Studies on the possibility of using these particles as a fluorescent cellular labeling agent and MRI contrast agent is presented.

Particle synthesis: Terbium-doped gadolinium oxide nanoparticles were synthesized by the polyol method. For the 5% Tb-doped nanocrystals, 5.7 mmol $GdCl_3$ and 0.3 mmol $TbCl_3$ were dissolved in 30 ml DEG, constantly stirred and heated in silicon oil bath at 140-160˚C for 1 h. Then, 7.5 mmol NaOH dissolved in 30 ml DEG was added. After complete dissolution of the reactants, the solution was refluxed at 180˚C for 4 h under stirring. For the 20% Tb-doped Gd_2O_3, the above procedure was followed, except for adding 1.1 mmol of $TbCl_3$ and no addition of NaOH. The synthesized suspensions were then filtered to remove large particles and agglomerations. Then the particles were functionalized with organic acids and PEG (see the manuscript for details).

Characterization: High-resolution transmission electron microscopy (HRTEM), x-ray photoelectron spectroscopy (XPS), energy disperse x-ray (EDX) and infrared spectra (IR) were carried out to characterize the synthesized material. Optical properties were characterized by photoluminescence (PL) measurements.

Cell labeling: A monocytic cell line, THP-1 cells, was differentiated to macrophage-like cells by treatment with phorbol 12-myristate 13-acetate (PMA). Cells were then incubated with Tb-doped particles and finally mounted on a Bio-Rad adhesion slide before fluorescence microscopy.

Relaxivity measurements: Proton relaxation times were measured with a 1.5 T Philips Achieva whole body scanner using the head coil. A 2D mixed multiecho SE interleaved with a multiecho IR sequence was used (see Paper 1 for details regarding imaging time parameters and other MRI settings).

Results and discussion:

Images of THP-1 cells incubated with DEG-capped particles (doped with 5% Tb), show bright yellow-green grains in the cytoplasm. Because the cells are highly phagocytic, these bright grains most probably correspond to particle containing endosomes or lysosomes.

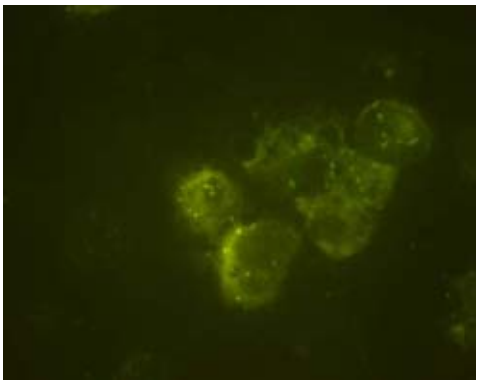

Figure 7. *Fluorescence microscopy image of THP-1 cells that have taken up 5% Tb doped Gd particles into endosomes or lysosomes.*

MRI relaxivity studies were performed with PEGylated Tb-containing Gd particles in water and compared with undoped Gd-PEG particles and a commercial agent, Gd-DTPA. The T_1 relaxivity of the different PEGylated particles was 2-3 times higher than Gd-DTPA. This indicates that there is a possibility to use lanthanide doped Gd_2O_3 particles as a multimodal MRI contrast agent.

Paper 3

Positive MRI Contrast Enhancement in THP-1 Cells with Gd_2O_3 Nanoparticles.

During the past decades MRI has become a well established technique for clinical diagnosis and the use of contrast agents to obtain improved images has played a great role for the increased utility of MRI. In this study we examine nanoparticles of Gd_2O_3 as a cell labeling contrast agent for MRI.

Particle synthesis: Nanoparticles of Gd_2O_3 were synthesized by the polyol method. $GdCl_3$ was dissolved in 10 ml DEG (diethylene glycol) by heating the mixture to 140˚C. Solid NaOH was dissolved in 5 ml DEG and subsequently added to the Gd solution. The temperature was then raised to 180˚C and held constant for 4 h under reflux and magnetic stirring, yielding a colloid. This particle solution was filtered and dialyzed to exclude large particles and ions.

Characterization: The particles were characterized by high-resolution electron microscopy (TEM) and photoelectron spectroscopy (XPS).

Cell labeling: THP-1 monocytes were incubated in different concentrations of Gd_2O_3 for 2 h at 37˚C in 5% CO_2 atmosphere. After incubation cells were washed and prepared for MRI measurements. In addition, cell viability after incubation with Gd_2O_3 for different period of times was studied with typan blue coloring/bürker chamber counting.

Relaxivity measurements: Cell samples were measured with a Philips Achieva 1.5 T MR-scanner using the head coil. T_1 was measured with inversion recovery pulse sequence with TE=29 ms, TR=3000 ms (for samples with Gd incubation conc. 1.0-2.5 mM) and IR=50-2900 ms (9 measure points). The 0.5 mM (incubation conc.) sample was measured with TR=10000 ms and IR=50-5000 ms (10 measure points). T_2 was

measured with a multi echo sequence, TE=20 ms, TR=1000 ms, number of echoes were 16 and the flip angle was 70 deg. FOV for the measurements was 200 mm and slice thickness was 5 mm.

Relaxivity results and discussion: Relaxivity results show that intracellular Gd_2O_3 shorten relaxation times with increasing concentration. For r_1, the relaxivity of particles in monocytes was not significantly different compared to particles in cell culture medium (p=0.36). For r_2, the relaxivity between samples in monocytes and samples in cell culture medium was significantly different (p=0.02). For monocyte samples r_1 was 4.1 s^{-1} mM^{-1} and r_2 was 17.4 s^{-1} mM^{-1}. Corresponding r_1 and r_2 for particles in medium were 3.6 s^{-1} mM^{-1} and 12.9 s^{-1} mM^{-1}, respectively.

Table 2. *Relaxivity constants (r_1, r_2) in s^{-1} mM^{-1}, standard deviation (SD), p-values and r_2/r_1 for Gd_2O_3 in cell culture medium and THP-1 cells.*

Relaxivity values Gd_2O_3-DEG

	r_1	SD	p	r_2	SD	p	r_2/r_1
RPMI 1640	3.6	±0.27	0.0009	12.9	±1.02	0.0062	3.5
THP-1 cells	4.1	±0.42	0.0023	17.4	±0.94	0.0003	4.2

This study indicates a potential for Gd_2O_3 nanoparticles to be used as a cell labeling contrast agent and signal intensity image shows high contrast enhancement for cell samples incubated with 1.5 mM Gd_2O_3. Cell viability after incubation observed in this study did not decrease to any significant degree.

6.2 Contributions by the author

Throughout my thesis work, I got the chance to collaborate interdisciplinary in a research network covering medicine, biology, chemistry and physics, which was both inspiring and productive. This resulted in me getting the chance to learn and understand more about other disciplines other than the biomedical field, which is my education background.

Paper 1

In this study, I was responsible for the study design and implementation of the MRI experimental setup, most of the laboratory work regarding this as well as the MRI measurements. I also analyzed and summarized the MRI results and figures for the manuscript. The synthesis and particle characterization was performed by our collaborators at the department for Physics, Chemistry and Biology at Linköping University.

Paper 2

I came up with the original idea of using undoped Gd material for, combined with the MRI studies, observing internalized particles using fluorescence microscopy. My first pilot study was then presented at ESMRMB in Basel in 2005. Our collaborators at the department of Physics, Chemistry and Biology had then started a project on doped Gd material and in the following work, which resulted in Paper 2, I was responsible for planning the cell studies regarding THP-1 cells. I did the laboratory work concerning these studies with DEG-particles and THP-1 cells, as well as the relaxivity

measurements and the manuscript writing for this part of the work.

Paper 3

I this study, I was responsible for the study design and implementation of the cell and MRI experiments. I did all the laboratory work regarding this and I also did all the MRI measurements and data analysis. In this work, our collaborators in chemistry and physics (at the department of Physics, Chemistry and Biology) did the synthesis, dialysis and characterization of the particles. I was responsible for summarizing these results as well as writing the major part of the manuscript and I was also responsible for correspondence with the journal.

Chapter 7
Discussion

The papers included in this thesis consider studies of different preparations of Gd_2O_3 nanoparticles for contrast enhancement in MRI. We have reported excellent relaxivity properties for Gd_2O_3 nanoparticles in different environments, such as water, buffers and cell culture medium as well as inside cells.

As noticed in these studies, Gd nanoparticles show increased relaxivity compared to commercial agent Gd-DTPA and have a T_1-reducing effect and a signal increase at low concentrations. It is here considered that the concentration range below 0.6 mM in plasma is most relevant for clinical use [36] and in our experiments, the Gd_2O_3 nanoparticles show high signal intensity below this concentration.

According to these results, the Gd_2O_3 particles in the size range of about 5-10 nm studied here, show paramagnetic behavior. They show high r_2 values and consequently higher r_2/r_1 quote in cells as well as in cell culture medium than for the particles in H_2O. This indicates that the T_2 effect is higher when the surroundings are not as homogeneous as in for instance water. Here, the water exchange may be altered as

the particles are captured in small enclosed compartments like the lysosomes/endosomes of cells. Also, in these compartments, as well as bound to for instance different proteins in the medium, the nanoparticles may act like larger particles, which would have greater effect on the transversal relaxivity than the longitudinal. However, we still observe a clear T_1 enhancement in T_1-weighted images. Going from having particles in aqueous solution to RPMI cell culture medium, for instance, both r_1 and r_2 increase. Macromolecular binding increases rotational correlation time which increases the relaxivity [37] and therefore, any proteins bound to particles in the RPMI-samples lead to higher relaxivity. However, since we observe this T_1 enhancement, although the very high r_2, Gd_2O_3 nanoparticles seem suitable for T_1 contrast enhancement.

Regarding the toxicity of gadolinium, it is clear that especially Gd^{3+} ions are toxic and could, for instance, block calcium channels, disturbing many actions achieved by Ca^{2+} [38]. Recently, it has also been suggested that gadolinium-based contrast agents could cause nephrogenic systemic fibrosis (NSF) in some patients [39]. It is therefore very important that the Gd_2O_3 nanoparticles are designed in such way that free Gd could not be released or stay in the circulation long enough to cause any tissue damage. In this thesis, the toxicity of Gd_2O_3 particles has only been studied as viability in cancer cells to confirm the methodology of the experiments, but these results were surprisingly good. During 8 days of exposure to Gd_2O_3, the viability of the cells did not decrease below acceptable levels for cell experiments. However, THP-1

is a tumor-transformed cell line and might perhaps have developed strategies for survival that normal cells do not have.

The major part of this thesis concerns pure Gd_2O_3 nanoparticles capped with DEG. Our interdisciplinary team involving research groups in medicine, biology, chemistry and physics, have performed and are currently performing several studies regarding capping and functionalization of these particles to make them non-toxic and clearable, although able to stay in circulation long enough to be detectable with MRI-techniques [40]. Work is also ongoing regarding whether to design a specific contrast agent to target certain tissue, for instance atherosclerotic plaques or stem cells. It has to be considered whether the particles should be coated to stay outside cells or if they should be designed to be an intracellular agent. When targeting stem cells, for instance to monitor stem cell migration, the agent is preferred to be able to get inside cells. Perhaps the particles should also be coated with organic fluorophores to get a bifunctional nanoparticle with both magnetic and luminescent properties [41]. For this reason, it is interesting to further investigate the Tb_3^+-doped particles.

Finally, the results of this thesis work suggest that doped Gd_2O_3 nanoparticles have contrast-enhancement as well as fluorescent properties that could open new diagnostic possibilities for designing a positive contrasted molecular imaging, multimodal agent. Such an agent can then be

considered as an MRI enhancer using common 1.5 T clinical systems, combined with different fluorescent techniques.

Bibliography

1. Klabunde KJ, Nanoscale Materials in Chemistry, Wiley-Interscience, New York, 2001.

2. Rao CNR, Kulkarni GU, Thomas PJ, Edwards PP, Size-Dependent Chemistry: Properties of Nanocrystals, *Chemistry*, 2002; 8: 28-35.

3. Pankhurst QA, et al., Applications of Magnetic Nanoparticles in Biomedicine, *J Phys D: Appl Phys,* 2003; 36: R167-R181.

4. Tartaj P, et al., The Preparation of Magnetic Nanoparticles for Applications in Biomedicine, *J Phys D: Appl Phys,* 2003; 36: R182-R197.

5. Berry CC, Curtis ASG, Functionalisation of Magnetic Nanoparticles for Applications in Biomedicine, *J Phys D: Appl Phys,* 2003; 36: R198-R206.

6. Reimer P, et al., Clinical MR Imaging, Springer Verlag, Berlin, 2003.

7. Hendrick RE, Haacke EM, Basic Physics of MR Contrast Agnets and Maximization of Image Contrast, *J Magn Res Im,* 1993; 3: 137-148.

8. McDonald MA, Watkin KL, Investigations into the Physicochemical Properties of Dextran Small Particulate Gadolinium Oxide Nanoparticles, *Acad Radiol,* 2006; 13: 421-427.

9. Brown M, Semelka RC, MRI; Basic Principles and Applications, Wiley-Liss, New York, 1999.

10. Wehrli FW, Shaw D, Kneeland JB, Biomedical Magnetic Resonance Imaging. Principles, Methodology and Applications, VCh Publishers, New York, 1988.

11. Gillies RJ, NMR in Physiology and Biomedicine, Academic Press, San Diego, 1994.

12. Rinck PA, Magnetic Resonance in Medicine, ABW Wissenschaftsverlag, Berlin, 2003.

13. Bjørnerud A, Proton Relaxation Properties of a Particulate Iron Oxide MR Contrast Agent in Different Tissue Systems, Dissertation No. 1160, Uppsala University, Sweden, 2002, ISBN 91-554-5330-9.

14. Friman O, Asaptive Analysis of Functional MRI Data, Dissertation No. 836, Linköping University, Sweden, 2003, ISBN 91-7373-699-6.

15. Mitchell DG, Cohen M, MRI Principles, Saunders, Elsevier, Philadelphia, 2004.

16. Bernstein MA, King KF, Zhou XJ, Handbook of MRI Pulse Sequences, Elsevier Academic Press, Burlington, 2004.

17. Lombardi M et al., Use of the Mean Transit Time of an Intravascular Contrast Agent as an Exchange-Intensitive Index of Myocardial Perfusion, *J Magn Res Im,* 1999; 9: 402-408.

18. Mathur de Vré R, Lemort M, Biophysical Properties and Clinical Applications of Magnetic Resonance Imaging Contrast Agents, *Br J Radiol,* 1995; 68: 225-247.

19. Greenwood NN, Chemistry of the Elements, Reed Educational and Professional Publishing, Oxford, 1997.

20. Enghag P, Jordens grundämnen och deras upptäckt, Industrilitteratur, Stockholm, 1998.

21. ”Gadolinium” in Swedish National Encyclopedia, http://www.ne.se/html/about_ne_eng.jsp, retrieved 2007-09-10.

22. Frank JA, Anderson SA, Kalsih H, Jordan EK, Lewis BK, Yocum GT, Arbab AS, Methods for Magnetically Labeling Stem and Other Cells for Detection by *in vivo* Magnetic Resonance Imaging, *Cytotherapy,* 2004; 6: 621-625.

23. Raymond N, Pierre VC, Next Generation, High Relaxivity Gadolinium MRI Agents, *Bioconj Chem,* 2005; 16: 3-8.

24. Koenig SH, Kellar KE, Theory of $1/T_1$ and $1/T_2$ NRMD Profiles and Solutions of Magnetic Nanoparticles, *Magn Res Med,* 1995; 34: 227-233.

25. Engström M, Klasson A, Pedersen H, Vahlberg C, Käll P-O, Uvdal K, High Proton Relaxivity for Gadolinium Oxide Nanoparticles, *MAGMA,* 2006; 19: 180-186.

26. Cunningham CH, Arai T, Yang PC, McConnell MV, Pauly JM, Conolly SM, Positive Contrast Magnetic Resonance Imaging of Cells Labeled with Magnetic Nanoparticles, *Magn Res Med,* 2005; 53: 999-1005.

27. "THP-1" in European Collection of Cell Cultures, http://www.ecacc.org.uk, retrieved 2008-01-25.

28. Tsuchiya S, Yamabe M, Yamaguchi Y, Kobayashi Y, Konno T, Tada K, Establishment and Characterization of a Human Acute Monocytic Leukemia Cell Line (THP-1), *Int J Cancer,* 1980; 26: 171-176.

29. Auwerx J, The Human Leukemia Cell Line, THP-1: a Multifacetted Model for the Study of Monocyte-Macrophage Differentiation, *Experentia,* 1991; 47: 22-31.

30. Ziess homepage, http://www.zeiss.com/c1256b5e0047ff3f/Contents-Frame/52c01f2588066339c1256c3e003669f0, retrieved 2007-08-17.

31. Atkins P, de Paula J, Atkins' Physical Chemistry, Oxford University Press, New York, 2002.

32. Massoud TF, Gambhir SS, Molecular Imaging in Living Subjects: Seeing Fundamental Biological Processes in a New Light, *Genes Dev,* 2003; 17: 545-580.

33. Santra S, Bagwe RP, Dutta D, Stanley JT, Walter GA, Tan W, Moudgil BM, Mericle RA, Synthesis and Characterization of Fluorescent, Radio-Opaque and Paramagnetic Silica

Nanoparticles for Multimodal Bioimaging Applications, *Adv Mater,* 2005; 17: 2165-2169.

34. Kircher MF, Mahmood U, King RS, Weissleder R, Josephson L, A Multimodal Nanoparticle for Preoperative Magnetic Resonance Imaging and Intraoperative Optical Brain Tumor Delineation, *Cancer Res,* 2003; 63: 8122-8125.

35. Goldys EM, Drozdowicz-Tomsia K, Jinjun S, Dosev D, Kennedy IM, Yatsunenko S, Godlewski M, Optical Characterization of Eu-doped and Undoped Gd_2O_3 Nanoparticles Synthesized by the Hydrogen Flame Pyrolysis Method, *J Am Chem Soc,* 2006; 128: 14498-14505.

36. Fass, the official Swedish pharmacology information portal, http://www.fass.se/LIF/home/index.jsp?UserTypeID=0, retrieved 2008-01-25.

37. Lauffer RB, Paramagnetic Metal Complexes as Water Proton Relaxation Agents for NMR imaging: Theory and Design, *Chem Rev,* 1987: 87: 901-927.

38. Pałasz A, Czekaj P, Toxicological and Cytophysiological Aspects of Lanthanides Action, *Acta Biochim Pol,* 2000; 47: 1107-1114.

39. Kuo PH, Gadolinium-Containing MRI Contrast Agents: Important Variations on a Theme for NSF, *J Am Coll Radiol,* 2008; 1: 29-35.

40. Fortin MA, Petoral JM Jr, Söderlind F, Klasson A, Engström M, Veres T, Käll P-O, Uvdal K, Polyethylene Glycol-Covered Ultra-Small Gd_2O_3 Nanoparticles for Positive Contrast at 1.5 T Magnetic Resonance Clinical Scanning, *Nanotechnology,* 2007; 18: 1-9.

41. Bridot J-L, Faure A-C, Laurent S, Rivière C, Billotey C, Hiba B, Janier M, Josserand V, Coll J-L, Vander Elst L, Muller R, Roux S, Perriat P, Tillement O, Hybrid Gadolinium Oxide Nanoparticles: Multimodal Contrast Agents for *in vivo* Imaging, *J Am Chem Soc,* 2007; 129: 5076-5084.